

JAERI-Review  
2002-037



JP0350008



ABSTRACTS OF THE WORKSHOP ON ORBITAL ORDERING  
AND FLUCTUATIONS IN d-AND f-ELECTRON SYSTEMS  
MARCH 4-6, 2002, ASRC, JAERI, TOKAI, JAPAN

December 2002

(Eds.) Kazuo UEDA and Takashi HOTTA

日本原子力研究所  
Japan Atomic Energy Research Institute

本レポートは、日本原子力研究所が不定期に公刊している研究報告書です。  
入手の問い合わせは、日本原子力研究所研究情報部研究情報課（〒319-1195 茨城県那珂郡東海村）あて、お申し越し下さい。なお、このほかに財団法人原子力弘済会資料センター（〒319-1195 茨城県那珂郡東海村日本原子力研究所内）で複写による実費頒布を行っております。

This report is issued irregularly.  
Inquiries about availability of the reports should be addressed to Research Information Division, Department of Intellectual Resources, Japan Atomic Energy Research Institute, Tokai-mura, Naka-gun, Ibaraki-ken 〒319-1195, Japan.

**Abstracts of the Workshop on  
Orbital Ordering and Fluctuations in d- and f-electron Systems**

March 4-6, 2002, ASRC, JAERI, Tokai, Japan

(Eds.) Kazuo UEDA and Takashi HOTTA

Advanced Science Research Center  
(Tokai Site)  
Japan Atomic Energy Research Institute  
Tokai-mura, Naka-gun, Ibaraki -ken

(Received October 8, 2002)

Strongly correlated f- and d-electron systems including heavy Fermion systems and transition metal oxides are important source of exciting new phenomena in condensed matter physics. Recently it has been recognized in more profound way that the orbital degeneracy of the f- and d-electrons plays very important role underlying those exotic phenomena. The idea of the present workshop is to bring active researchers in the field together and to exchange ideas in informal atmosphere. In the workshop, twenty seven papers were presented and the following subjects were discussed : orbital ordering in transition metal oxides, role of orbital degeneracy in heavy Fermion systems and effect of geometrical frustration on orbital fluctuations.

**Keywords:** Orbital Ordering, Orbital Fluctuations, Electron Correlation, Unconventional Superconductivity, Novel Magnetism, d-electron Systems, f-electron Systems.

# 「d-および f-電子系における軌道秩序と揺らぎ」

## ワークショップ要旨集

2002年3月4日-6日、東海研究所

日本原子力研究所先端基礎研究センター

(編) 上田 和夫・堀田 貴嗣

(2002年10月8日 受理)

重い電子系や遷移金属酸化物などの強相関 f あるいは d-電子系は、物性物理学における新しい現象の源泉になっている。最近、こうした従来の常識では理解できない新しい現象の背後に、f あるいは d-電子の持つ軌道の自由度が重要な働きをしているのではないかということが、これまでに深く認識されるようになってきた。会議では口頭、ポスターあわせて27の発表があり、遷移金属酸化物における軌道秩序、重い電子系における軌道自由度の役割、幾何学的フラストレーションと軌道ゆらぎの関連などが議論された。

---

日本原子力研究所（東海駐在）：〒319-1195 茨城県那珂郡東海村白方白根 2-4

本ワークショップの世話人は、日本原子力研究所先端基礎研究センター 上田和夫、堀田貴嗣が担当した。

## Contents

Program of the Workshop on “Orbital Ordering and Fluctuations in d- and f-electron Systems” .....	1
1. Physics of Ruthenates: the Charge, the Spin and the Orbital .....	5
M. Sigrist (ETH, Zurich)	
2. Magnetic Frustration and Criticality at the Structural Instability in $\text{Ca}_{2-x}\text{Sr}_x\text{RuO}_4$ : the Role of the Orbital Degree of Freedom .....	6
S. Nakatsuji (NHMFL, FSU)	
3. Orbital Correlations and Charge Dynamics in Manganites .....	7
T. Kimura (Tokyo)	
4. Orbital Dynamics in 3d Transition Metal Oxides .....	8
S. Ishihara (Tokyo)	
5. Spin and Orbital Effects of Cooper Pairs Coupled to a Single Magnetic Impurity .....	9
M. Koga (Shizuoka)	
6. Microscopic Theory on the Spin-orbit Coupling and Triplet Superconductivity in $\text{Sr}_2\text{RuO}_4$ .....	10
Y. Yanase (Tokyo)	
7. Orbital Ordering in Manganites and Ruthenates .....	11
T. Hotta (ASRC, JAERI)	
8. Transfer Matrix Renormalization Group Method and its Applications ..	12
X. Wang (ITP, Chinese Academy of Sciences)	
9. DMRG Study of 2D Electrons in Magnetic Field .....	13
N. Shibata (Tokyo)	

10.	<b>Fermi Surface Nesting in the Filled Skutterudite Compounds</b> .....	14
	H. Harima (ISIR, Osaka)	
11.	<b>Fermi Surface of Magnetic Uranium Compounds in Relativistic Spin-polarized Band Theory</b> .....	15
	H. Yamagami (Kyoto Sangyo Univ.)	
12.	<b>Density Functional Approach with an Explicitly Orbital-dependent Exchange and Correlation Energy Functional</b> .....	16
	M. Higuchi (Tohoku)	
13.	<b>Electronic Structure and the Fermi Surface of UFeGa<sub>5</sub></b> .....	17
	T. Maehira (ASRC, JAERI)	
14.	<b>NMR Studies of Magnetism and Unconventional Superconductivity in CeMIn<sub>5</sub></b> .....	18
	Y. Kitaoka(Osaka)	
15.	<b>Spin Fluctuation Induced Superconductivity Controlled by Orbital Fluctuation</b> .....	19
	T. Takimoto (ASRC, JAERI)	
16.	<b>Superconductivity in CeMIn<sub>5</sub> and Related Compounds</b> .....	20
	J. Thompson (Los Alamos)	
17.	<b>Superconducting Gap Structure of Heavy-fermion Superconductor CeCoIn<sub>5</sub></b> .....	21
	K. Izawa (ISSP, Tokyo)	
18.	<b>Low Temperature Magnetization of CeTIn<sub>5</sub> (T=Co and Ir)</b> .....	22
	T. Tayama (ISSP, Tokyo)	
19.	<b>Photoemission Study of CeTIn<sub>5</sub> (T=Rh and Ir)</b> .....	23
	S. Fujimori (Spring-8, JAERI)	

20.	<b>Analysis of Superconductivity in <math>\text{Sr}_2\text{RuO}_4</math> on the Basis of the Six-band Hubbard Model</b> .....	24
	S. Koikegami (JST, AIST)	
21.	<b>Perturbation Theory on the Superconductivity of Heavy Fermion Superconductors <math>\text{CeIr}_x\text{Co}_{1-x}\text{In}_5</math></b> .....	25
	Y. Nishikawa (Kyoto)	
22.	<b>Kondo Hole in One-dimensional Kondo Insulators</b> .....	26
	I. Maruyama (ISSP, Tokyo)	
23.	<b>Heavy Fermion Behavior and Orbital Fluctuations in <math>\text{LiV}_2\text{O}_4</math></b> .....	27
	Y. Yamashita (ISSP, Tokyo)	
24.	<b>Spin-Peierls Transition in <math>S=1</math> Antiferromagnetic Heisenberg Chain with Spin-phonon Coupling</b> .....	28
	H. Onishi (Osaka)	
25.	<b>Magnetic Properties of <math>\text{UNiGa}_5</math> and <math>\text{UPtGa}_5</math></b> .....	29
	Y. Tokiwa (ASRC, JAERI)	
26.	<b>Ga NMR/NQR Study of <math>\text{UTGa}_5</math> (<math>T=\text{Pt}</math> and <math>\text{Ni}</math>)</b> .....	30
	H. Kato (ASRC, JAERI)	
27.	<b>Superconductivity in a Pyrochlore Oxide <math>\text{Cd}_2\text{Re}_2\text{O}_7</math></b> .....	31
	H. Sakai (ASRC, JAERI and Kyoto Univ.)	

## 目 次

「d-およびf-電子系における軌道秩序と揺らぎ」ワークショッププログラム	1
1. ルテニウム酸化物の物理：電荷、スピン、軌道	5
M. Sigrist (スイス連邦工科大学)	
2. $\text{Ca}_{2-x}\text{Sr}_x\text{RuO}_4$ の構造不安定点における臨界性と磁気フラストレーション：軌道自由度の役割	6
中辻 悟 (フロリダ州立大学・国立高磁場研究所)	
3. マンガン酸化物における軌道相関と電荷ダイナミクス	7
木村 剛 (東京大学)	
4. 軌道秩序のある3d遷移金属酸化物における軌道ダイナミクス	8
石原 純夫 (東京大学)	
5. 単一磁気不純物と結合するクーパー対に対するスピン・軌道効果	9
古賀 幹人 (静岡大学)	
6. $\text{Sr}_2\text{RuO}_4$ におけるスピン・軌道相互作用とトリプレット超伝導に対する微視的理論	10
柳瀬 陽一 (東京大学)	
7. マンガン酸化物およびルテニウム酸化物における軌道秩序	11
堀田 貴嗣 (原研先端基礎)	
8. 転送行列繰り込み群法とその応用	12
X. Wang (中国科学院理論物理研究所)	
9. 磁場下2次元電子の密度行列繰り込み群法による研究	13
柴田 尚和 (東京大学)	



10. 充填スクッテルダイト化合物におけるフェルミ面ネスティング .....	14
播磨尚朝 (大阪大学・産業科学研究所)	
11. 相対論的スピン分極バンド理論における磁性ウラン化合物の フェルミ面 .....	15
山上 浩志 (京都産業大学)	
12. あらわな軌道依存性のある交換相関エネルギーを考慮した 密度汎関数アプローチ .....	16
樋口 雅彦 (東北大学)	
13. UFeGa <sub>5</sub> の電子構造とフェルミ面 .....	17
眞榮平 孝裕 (原研先端基礎)	
14. CeMIn <sub>5</sub> における磁性と超伝導に対する NMR による研究 .....	18
北岡 良雄 (大阪大学)	
15. 軌道揺らぎによって制御されるスピン揺らぎ起源の超伝導 .....	19
瀧本 哲也 (原研先端基礎)	
16. CeMIn <sub>5</sub> と関連物質における超伝導 .....	20
J. Thompson (ロスアラモス研究所)	
17. 重い電子系超伝導 CeCoIn <sub>5</sub> の超伝導ギャップ構造 .....	21
井澤 公一 (東京大学物性研究所)	
18. CeTIn <sub>5</sub> (T=Co, Ir) の低温磁化 .....	22
田山 孝 (東京大学物性研究所)	
19. CeTIn <sub>5</sub> (T=Rh, Ir) の光電子分光による研究 .....	23
藤森 伸一 (原研・Spring-8)	
20. 6 バンドハバード模型に基づく Sr <sub>2</sub> RuO <sub>4</sub> の超伝導の解析 .....	24
小池上 繁 (産総研)	

21. 重い電子系物質 $\text{CeIr}_x\text{Co}_{1-x}\text{In}_5$ の超伝導に対する擾動論的研究 .....	25
西川 裕規 (京都大学)	
22. 1次元近藤絶縁体における近藤ホール .....	26
丸山 勲 (東京大学物性研究所)	
23. $\text{LiV}_2\text{O}_4$ における重い電子的振る舞いと軌道揺らぎ .....	27
山下 靖文 (東京大学物性研究所)	
24. スピン格子結合をもつ $S=1$ 反強磁性ハイゼンベルグ鎖におけるスピン・ パイエルズ転移 .....	28
大西 弘明 (大阪大学)	
25. $\text{UNiGa}_5$ および $\text{UPtGa}_5$ の磁氣的性質 .....	29
常盤 欣文 (原研先端基礎)	
26. $\text{UTGa}_5$ ( $T=\text{Pt, Ni}$ ) の Ga NMR/NQR による研究 .....	30
加藤 治一 (原研先端基礎)	
27. パイロクロア酸化物 $\text{Cd}_2\text{Re}_2\text{O}_7$ の超伝導 .....	31
酒井 宏典 (原研先端基礎)	

Workshop on  
“Orbital Ordering and Fluctuations in d- and f-electron systems”

*Advanced Science Research Center*  
*Japan Atomic Energy Research Institute*  
*March 4-6, 2002*

**2002.3.4 (Monday)**

12:00- registration

*Opening*

13:25-13:30 K. Ueda (ISSP, Tokyo and ASRC, JAERI)

*Transition Metal Oxides (I)*

*Chair: T. Hotta*

13:30-14:30 M. Sigrist (ETH, Zurich)

Physics of ruthenates: the charge, the spin and the orbital

14:30-15:30 S. Nakatsuji (NHMFL, FSU)

Magnetic frustration and criticality at the structural instability in  
 $\text{Ca}_{2-x}\text{Sr}_x\text{RuO}_4$ : the role of orbital degree of freedom

15:30-15:45 Coffee break

*Transition Metal Oxides (II)*

*Chair: M. Sigrist*

15:45-16:15 T. Kimura (Tokyo)

Orbital correlations and charge dynamics in manganites

16:15-16:45 S. Ishihara (Tokyo)

Orbital dynamics in orbital ordered 3d transition metal oxides

16:45-17:00 M. Koga (Shizuoka)

Spin and Orbital Effects of Cooper Pairs Coupled to a Single Magnetic  
Impurity

17:00-17:15 Y. Yanase (Tokyo)

Microscopic theory on the spin-orbit interaction and the triplet  
superconductivity in  $\text{Sr}_2\text{RuO}_4$

17:15-17:30 T. Hotta (ASRC, JAERI)  
Orbital Ordering in Manganites and Ruthenates

*2002.3.5 (Tuesday)*

*DMRG*

*Chair: K. Ueda*

9:00-10:00 X. Wang (ITP, Chinese Academy of Sciences)  
Transfer Matrix Renormalization Group Method and its applications

10:00-10:30 N. Shibata (Tokyo)  
DMRG study of 2D electrons in magnetic field

10:30-10:50 Coffee break

*Discussion (I)*

*coordinator: T. Hotta*

10:50-11:50 free discussion on transition metal oxides

11:50-13:20 Lunch

*Band-structure Calculation*

*Chair: T. Moriya*

13:20-13:50 H. Harima (ISIR, Osaka)  
Fermi surface nesting in the filled skutterudite compounds

13:50-14:20 H. Yamagami (Kyoto Sangyo Univ.)  
Fermi surface of magnetic uranium compounds in relativistic spin-polarized band theory

14:20-14:45 M. Higuchi (Tohoku)  
Density functional approach with an explicitly orbital-dependent exchange and correlation energy functional

14:45-15:00 T. Maehira (ASRC, JAERI)  
Electronic structure and the Fermi surface of  $UFeGa_5$

15:00-15:15 Coffee break

***Ce-115(I)***

*Chair: T. Sakakibara*

- 15:15-16:15 K. Kitaoka (Osaka)  
NMR Studies of magnetism and unconventional superconductivity  
in CeMIn<sub>5</sub>
- 16:15-16:30 T. Takimoto (ASRC, JAERI)  
Spin Fluctuation Induced Superconductivity Controlled by Orbital  
Fluctuation
- 16:30-17:30 Poster
- 18:30-20:30 Banquet

***2002.3.6 (Wednesday)***

***Ce-115(II)***

*Chair: R. E. Walstedt*

- 9:00-10:00 J. Thompson (Los Alamos)  
Superconductivity in CeMIn<sub>5</sub> and Related Compounds
- 10:00-10:15 K. Izawa (ISSP, Tokyo)  
Superconducting Gap Structure of Heavy-Fermion superconductor  
CeCoIn<sub>5</sub>
- 10:15-10:30 T. Tayama (ISSP, Tokyo)  
Low Temperature Magnetization of CeTIn<sub>5</sub> (T=Co and Ir)
- 10:30-10:50 Coffee break

***Discussion (I)***

*coordinator: K. Ueda*

- 10:50-11:50 free discussion on Ce-115 system

***Closing***

- 11:50-12:00 H. Yasuoka (ASRC, JAERI)

*Poster presentation*

1. S. Fujimori (Spring-8, JAERI)  
Photoemission study of  $\text{CeTIn}_5$  (T=Rh and Ir)
2. S. Koikegami (JST, AIST)  
Analysis of superconductivity in  $\text{Sr}_2\text{RuO}_4$  on the basis of the six-band Hubbard model
3. Y. Nishikawa (Kyoto)  
Perturbation Theory on the Superconductivity of Heavy Fermion Superconductor  $\text{CeIr}_x\text{Co}_{1-x}\text{In}_5$
4. I. Maruyama (ISSP, Tokyo)  
Kondo hole in one-dimensional Kondo insulators
5. Y. Yamashita (ISSP, Tokyo)  
Heavy Fermion Behavior and Orbital Fluctuation in  $\text{LiV}_2\text{O}_4$
6. H. Onishi (Osaka)  
Spin-Peierls transition in S=1 antiferromagnetic Heisenberg chain with spin-phonon coupling
7. Y. Tokiwa (ASRC, JAERI)  
Magnetic Properties of  $\text{UNiGa}_5$  and  $\text{UPtGa}_5$
8. H. Kato (ASRC, JAERI)  
Ga NMR/NQR study of  $\text{UTGa}_5$  (T=Pt and Ni)
9. H. Sakai (ASRC, JAERI and Kyoto Univ.)  
Superconductivity in a pyrochlore oxide  $\text{Cd}_2\text{Re}_2\text{O}_7$

# 1. Physics of ruthenates: the charge, the spin and the orbital

Manfred Sigrist

*Theoretische Physik, ETH-Hönggerberg, 8093 Zürich, Switzerland*

Ruthenates have received much attention for their versatile physics. In this talk I will review some aspects of the unconventional superconductivity of the quasi-two-dimensional Fermi liquid  $\text{Sr}_2\text{RuO}_4$ . The superconducting phase has spin-triplet p-wave symmetry and violates time reversal (chiral p-wave phase), an analog to the A-phase of superfluid  $^3\text{He}$ . For the stability of this phase spin-orbit coupling and the relation among the three  $4d-t_{2g}$ -conduction bands are important. This requires that  $d_{xy}$ -band is dominant for superconductivity. In this context the problem of orbital-dependent superconductivity will be discussed. A further unusual property is the occurrence of inhomogeneous superconductivity in  $\text{Sr}_2\text{RuO}_4$  with Ru-metal inclusions at  $T \approx 3\text{K}$  ("3-Kelvin phase"). This phase provides an interesting means to test the pairing symmetry.

If the isoelectronic Ca replaces Sr, i.e.  $\text{Ca}_2\text{RuO}_4$ , we find an antiferromagnetic Mott-insulator. The continuous doping between the two limits,  $\text{Ca}_{2-x}\text{Sr}_x\text{RuO}_4$ , leads to a sequence of phases with unusual properties. I will show that some of the phases can be understood within the concept of an orbital-selective Mott insulator transition. In contrast to the superconductor, here the other two  $t_{2g}$ -orbitals,  $d_{yz}$  and  $d_{zx}$ , are the key players. Together they contain 3 localized electrons while the  $d_{xy}$ , though half-filled, retains its itinerant character. This leads to an orbital and spin degree of freedom whose dynamics can be described within Kugel-Khomskii-like effective Hamiltonian. A mean field calculation shows that such a model explains the essential properties of  $\text{Ca}_{2-x}\text{Sr}_x\text{RuO}_4$ , at intermediate doping.

The work reported here has been done in collaboration with T.M. Rice, D. Agterberg, K.K. Ng, J. Goryo, M. Matsumoto, A. Furusaki, H. Monien, H. Kusunose, C. Honerkamp, V. Anisimov, M. Troyer, I. Nekrasov and D. Kondakov.

2. Magnetic frustration and criticality at the structural instability in  $\text{Ca}_{2-x}\text{Sr}_x\text{RuO}_4$ :  
the role of the orbital degree of freedom

Satoru Nakatsuji

National High Magnetic Field Laboratory, Tallahassee, Florida 32310 USA

In strongly correlated multi-band systems, the deformation of lattice, which strongly couples with orbital degrees of freedom, often dramatically alters the ground state. Among them, the single layered ruthenate  $\text{Ca}_{2-x}\text{Sr}_x\text{RuO}_4$  gives a unique example, connecting two distinct ground states: the Mott insulator  $\text{Ca}_2\text{RuO}_4$  and the spin-triplet superconductor  $\text{Sr}_2\text{RuO}_4$ . The isovalent Sr substitution changes the crystal distortions to induce the Mott transition and the rich evolution of itinerant magnetism. This talk will review the phase diagram and feature the role of Ru 4d orbital degrees of freedom.



### 3. Orbital correlations and charge dynamics in manganites

Tsuyoshi Kimura

*Department of Applied Physics, University of Tokyo, Bunkyo-ku, Tokyo 113-8656*

The orbital degree of freedom of d-electrons in manganites plays an important role not only in the magnetic structure/property but also in the charge dynamics. In analogy to localized spins coupled with the conduction electron spin, the orbital ordering and correlation occasionally govern the anisotropy and magnitude of the electron transfer in manganites. We present the results of recent structural, magnetic, electric, and spectroscopic investigations on the interaction between the orbital and charge dynamics for perovskite manganites.

This work has been done in collaboration with K. Tobe, K.T. Takahashi, K. Hatsuda, S. Kawamoto, and Y. Tokura.

## 4. Orbital Dynamics in 3d Transition Metal Oxides

Sumio Ishihara

Department of Applied Physics,  
University of Tokyo, Tokyo 113-8656 Japan

Experimental and theoretical studies of orbital degree of freedom in 3d transition metal oxides have started long time ago. It was considered widely that the static orbital order and the cooperative lattice distortion are indivisibility with each other, although it is recently found that the orbital orderings in some classes of materials are not accompanied with the compatible lattice distortions. On the other hand, differences between the two are expected to appear clearly in their dynamics, because of difference of their characteristic energies.

I will introduce, in this talk, the recent theoretical developments of orbital dynamics in 3d transition metal oxides. The collective orbital excitation in the orbital ordered phase is termed orbital wave and its quantized object is “orbiton”. This new type of excitation has been predicted theoretically and recently observed by Raman scattering in  $\text{LaMnO}_3$ . Now, orbiton is surveyed in a wide variety of 3d transition metal oxides with orbital degeneracy. Perovskite titanates and vanadates are one of the candidates. One and two electrons occupy the triply degenerate  $t_{2g}$  orbitals in  $\text{Ti}^{3+}$  and  $\text{V}^{3+}$  ions, respectively. There are several different characters between  $e_g$  and  $t_{2g}$  orbitals, such as a number of degeneracy, the orthogonality of the transfer integral, the orbital angular momentum and so on. It is shown, in the linear spin wave approximation, that there exist two kinds of excitations per ions, i.e. a dispersive excitation mode and a non-dispersive zero-energy mode. By including the zero-point fluctuation in the antiferro-type orbital ordered state, a stable orbital state is obtained. Possible excitation processes of orbital wave in the Raman scattering and the neutron scattering experiments are proposed, and their spectra are calculated.

This work is in collaboration with T. Hatakeyama and S. Maekawa in Institute for Materials Research, Tohoku University.

### References

- [1] S. Ishihara, T. Hatakeyama and S. Maekawa *Phys. Rev. B* **65** 064442 (2002).
- [2] S. Ishihara and S. Maekawa (unpublished).

## 5. Spin and Orbital Effects of Cooper Pairs Coupled to a Single Magnetic Impurity

Mikito Koga<sup>1</sup> and Masashige Matsumoto<sup>2</sup>

<sup>1</sup>Fac. of Edu. and <sup>2</sup>Fac. of Sci., Shizuoka Univ.

We focus on two simple unconventional superconducting states which have a full energy gap and whose angular momenta are good quantum numbers, assuming that a local spin is located at the center of two-dimensional coordinates. One is a  $p_x + ip_y$ -wave state whose order parameter is given by  $\Delta_{\uparrow\downarrow}(k_x + ik_y)$ , and the other is a  $d_{x^2-y^2} + id_{xy}$ -wave one represented by  $\Delta_{\uparrow\downarrow}([k_x^2 - k_y^2] + ik_x k_y)$ . Since the density of quasiparticle states for both cases has the same energy gap with the  $s$ -wave, we can extract an orbital effect of Cooper pairs which is never seen in the  $s$ -wave superconductivity. We investigate a new type of Kondo effect due to a  $S_{\text{imp}} = 1/2$  or  $S_{\text{imp}} = 1$  impurity ( $S_{\text{imp}}$  is a size of the local spin) in these superconducting states, using the numerical renormalization group (NRG) method.

In our previous study on the Kondo effect in the unconventional superconductors [1,2], a short-range scattering object was considered for the impurity. The atomic orbital of the impurity is restricted to the  $s$ -orbital denoted by the  $l = 0$  angular momentum. The angular momentum of the Cooper pair is  $l = 1$  for the  $p_x + ip_y$ -wave and  $l = 2$  for the  $d_{x^2-y^2} + id_{xy}$ -wave. The NRG result shows that the ground state is a doublet and the situation is completely different from the  $s$ -wave superconducting case. However, in this case, we did not find any difference between the  $p_x + ip_y$ -wave and  $d_{x^2-y^2} + id_{xy}$ -wave cases.

In the present study [3], we take into account the scatterings of the  $l = 1$  ( $l = 2$ ) electrons on the impurity site as well as  $l = 0$  for the  $p_x + ip_y$ -wave ( $d_{x^2-y^2} + id_{xy}$ -wave). Introducing the two exchange couplings, we can distinguish the spin-triplet Cooper pair from the spin-singlet one in the Kondo effect. The difference appears in the form of the effective exchange interaction in our Kondo model. The  $p_x + ip_y$ -wave generates spin anisotropy, and the ground state is always a spin doublet for  $S_{\text{imp}} = 1/2$ . For  $S_{\text{imp}} = 1$ , the triplet state of the local spin is split into a singlet and a doublet, and the ground state is always a spin singlet. For the  $d_{x^2-y^2} + id_{xy}$ -wave, the ground state changes from a spin doublet to a particle-hole doublet as  $T_k$  increases for  $S_{\text{imp}} = 1/2$ . Similarly, the interchange of triplet and singlet ground states occurs for  $S_{\text{imp}} = 1$ .

1. M. Matsumoto and M. Koga: J. Phys. Soc. Jpn. **70** (2001) 2860.
2. M. Matsumoto and M. Koga: Phys. Rev. B **65** (2002) 024508.
3. M. Koga and M. Matsumoto: Phys. Rev. B (in press).

## 6. Microscopic Theory on the Spin-orbit Coupling and Triplet Superconductivity in $\text{Sr}_2\text{RuO}_4$

Youichi Yanase

Department of Physics, Graduate School of Science, University of Tokyo, 7-3 -1 Hongo  
Bunkyo-ku, Tokyo 113-0033, Japan

Triplet superconductivity in  $\text{Sr}_2\text{RuO}_4$  is investigated with main interest on the internal degree of freedom. The internal degree of freedom is an attractive character of the triplet superconductivity since various states are degenerate without spin-orbit coupling. The cooperation of the phenomenological theory [1] and experimental results [2] has concluded that the superconducting state in  $\text{Sr}_2\text{RuO}_4$  is characterized as  $\hat{d}(\mathbf{k}) = (k_x \pm ik_y)\hat{z}$  where  $\hat{d}$  is the D-vector. We perform a microscopic calculation to investigate how this state is realized by the spin-orbit coupling, and discuss the essential condition for it.

The starting model is the three band Hubbard Hamiltonian which represent  $4d_{xy}$ ,  $4d_{xz}$  and  $4d_{yz}$  orbitals in Ru ions. The on-site interaction including the intra-band coulomb  $U$ , inter-band coulomb  $U'$ , Hund coupling  $J_H$  and pair hopping  $J$  terms is taken into account. The effective interaction which gives an unconventional superconductivity is calculated by the perturbative method. The superconducting transition temperature is determined by solving the linearized Eliashberg equation. It is shown that the triplet superconductivity is obtained in sufficiently weak coupling region which justifies the perturbative method. The momentum dependence is  $p$ -wave, which is consistent with the result on the single band model [3]. An important result is that the orbital dependent superconductivity predicted by Agterberg *et al.* [4] robustly appears. Then, the superconducting transition is almost determined by one main band. The sixfold degeneracy is maintained unless the spin-orbit interaction is taken into account.

The effects of the spin-orbit interaction are classified into two kinds. One is the effect on the effective interaction. The other is the formation of new quasi-particles. We take both effects into account within the second order about the spin-orbit coupling. We find that this systematic treatment is necessary to obtain the correct results. It is shown that the cooperation between the spin-orbit interaction and the Hund coupling violate the  $\text{SU}(2)$  symmetry in the spin space, and determine the D-vector in the superconducting state. We investigate also the case of  $f$ -wave superconductivity by assuming the separable interaction in a main band.

The obtained results are summarized in Table 1. One of the main conclusion is that the D-vector along  $\hat{z}$  direction is obtained when the  $p$ -wave superconductivity occurs on the  $\gamma$ -band. Namely, the consistent result with experiments is microscopically derived in this case. On the other hand, inconsistent results are obtained in the other cases. These results gives a restriction on the microscopic mechanism of the triplet superconductivity.

	$\gamma$ -band	$\alpha$ -, $\beta$ -band
p-wave	$(k_x \pm ik_y)\hat{z}$	$k_y\hat{x} \pm k_x\hat{y}$
p-wave (with node)	none	$k_y\hat{x} \pm k_x\hat{y}$
f-wave	$(k_x^2 - k_y^2)(k_y\hat{x} \pm k_x\hat{y})$	$(k_x^2 - k_y^2)(k_x\hat{x} \pm k_y\hat{y})$

Table 1: Obtained superconducting state for each symmetry and main band.

- [1] M. Sgrist *et al.*: Physica C **317-318** (1999) 134.
- [2] G. M. Luke *et al.*: Nature **374** (1998) 558; K. Ishida *et al.*: Nature **376** (1998) 658.
- [3] T. Nomura and K. Yamada: J. Phys. Soc. Jpn. **69** (2000) 3678.
- [4] D. F. Agterberg, T. M. Rice and M. Sgrist: Phys. Rev. Lett. **78** (1997) 3374.

## 7. Orbital Ordering in Manganites and Ruthenates

Takashi Hotta

*Advanced Science Research Center  
Japan Atomic Energy Research Institute  
Tokai, Ibaraki 319-1195*

Recently it has been recognized that the orbital degree of freedom plays a crucial role in 3d and 4d transition metal oxides. Especially in manganites, orbital ordering has been considered as one of the key issues to understand the colossal magnetoresistance phenomenon beyond the standard double-exchange (DE) mechanism. Based on the DE model tightly coupled to Jahn-Teller phonons, the unexpected presence of stripes has been recently observed in the ferromagnetic phase [1]. These (diagonal) stripes are induced by the orbital degree of freedom, which forms a staggered  $x=0$  pattern in the background between stripes. A  $\pi$ -shift in the orbital order across stripes is identified, analogous to the  $\pi$ -shift in spin order across stripes in cuprates.

On the other hand, the layered ruthenate  $\text{Sr}_2\text{RuO}_4$  is known as a triplet superconductor, but when Sr is partially substituted by Ca, superconductivity is rapidly destroyed and a paramagnetic metallic phase appears. Upon further substitution, the system transforms into an antiferromagnetic insulator. The key role of the orbital degree of freedom to understand the magnetic properties of layered ruthenates is here discussed. In the G-type antiferromagnetic phase of  $\text{Ca}_2\text{RuO}_4$ , recent X-ray experiments reported the presence of 0.5 hole per site in the  $d_{xy}$  orbital, while the  $d_{yz}$  and  $d_{zx}$  orbitals contain 1.5 holes. This unexpected  $t_{2g}$  hole distribution is explained by a novel state with orbital ordering, stabilized by a combination of Coulomb interactions and lattice distortions [2]. In addition, the rich phase diagram presented here suggests the possibility of large magnetoresistance effects, and predicts a new ferromagnetic orbital-ordered phase in ruthenates.

[1] T. Hotta, A. Feiguin, and E. Dagotto, *Phys. Rev. Lett.* **86**, 4922 (2001).

[2] T. Hotta and E. Dagotto, *Phys. Rev. Lett.* **88**, 017201 (2002).

## **8. Transfer Matrix Renormalization Group Method and its applications**

Xiaoqun Wang

*Institute of Theoretical Physics, Chinese Academy of Sciences  
P.O. Box 2735, Beijing 100080, P.R. China*

I will present a review on transfer matrix formulation for density matrix renormalization group method. A brief introduction on density matrix renormalization group method is given with its key ideas and prospects. Its extension to the transfer matrix representation for quasi-one dimensional quantum systems is shown and a few of interesting applications are illustrated.

## 9. DMRG study of 2D electrons in magnetic field

Naokazu Shibata

*Dept. of Basic Science, Univ. of Tokyo, Komaba, Tokyo 153-8902, Japan*  
*+81-3-5454-6549, +81-3-5454-6998, shibata@phys.c.u-tokyo.ac.jp*

The electrons in two-dimensional systems are confined to the lowest Landau level under a high perpendicular magnetic field. In this limit, Laughlin proposed Jastrow-type ground state wave function at filling factors  $\nu = 1/q$  ( $q$  is an odd integer). This wave function is an exact zero-energy eigenstates of short-ranged repulsive interactions, and describes an incompressible liquid with an excitation gap, which explains fractional quantizations.

In weak magnetic fields, electrons occupy higher Landau levels. Since the filled Landau levels are inert, it will be a good approximation to consider only the partially occupied Landau level. Then naively we may think that the electrons in the partially filled level behave similarly to those in the partially filled lowest Landau level. However, this is not correct. The wave function in the higher Landau levels extends over a space with oscillations, and the interaction between them is more long-ranged. Therefore, the Laughlin state, that is the ground state for short-range interaction, ceases to be the good candidate for the ground state in the higher Landau levels, and the fractional quantum Hall state becomes unstable.

In the present study, we apply the density matrix renormalization group (DMRG) method to quantum hall systems, and calculate ground state wave function in high Landau levels (index  $N=1,2,3$ ). The obtained ground state electron-electron pair correlation functions show that various CDW states called stripe-phase, bubble-phase, and Wigner crystal are realized depending on the magnetic field. The boundary between the stripe and the bubble phases and that for the bubble phase and Wigner crystal are determined and each transitions are shown to be of first order[1].

### References

- [1] N. Shibata and D. Yoshioka: Phys. Rev. Lett. **86**, 5755, (2001).

## 10. Fermi surface nesting in the filled skutterudite compounds

Hisatomo HARIMA

*ISIR, Osaka University, Ibaraki, Osaka 567-0047*

The filled skutterudite with a general formula  $RT_4X_{12}$  ( $R$  = Rare earth, Th or U;  $T$  = Fe, Ru or Os;  $X$  = P, As or Sb) crystallizes in a unique BCC structure of a space group  $Im\bar{3}$  ( $T_h^5$ , #204). The compounds have recently attracted much attention as improved thermoelectric materials and for the variety of the electrical and magnetic properties. Among them,  $PrRu_4P_{12}$  shows a metal-insulator (M-I) transition at  $T_{MI} = 60$  K [1] and  $PrFe_4P_{12}$  undergoes a non-magnetic ordering at  $T_A = 6.5$  K [2], resulting in a low carrier system, which exhibits a heavy-fermion states in applied magnetic field [3]. The filled skutterudite compound  $PrT_4P_{12}$  ( $T$  = Fe/Ru) is an uncompensated metal with  $Pr^{3+}$ , then it could not be an insulator or a semi-metal within the same primitive unit cell. The study of Fermi surface reveals that the main Fermi surface of  $LaFe_4P_{12}$  is a distorted cube and the volume is almost a half of the BCC BZ with a sharp peak in the density of states, indicating that the nesting with  $q = (1, 0, 0)$  is likely in the skutterudite compounds. [4] In fact, structural phase transitions with  $q = (1, 0, 0)$  are observed below  $T_{MI}$  and  $T_A$  in  $PrRu_4P_{12}$  [5] and  $PrFe_4P_{12}$  [6], respectively. These experiments show that the unit cell becomes doubled from BCC to simple lattice, then they could be a semi-metal or an insulator, though the atomic displacements remain undetermined experimentally.

We have performed bandstructure calculations for the doubled unit cell (34 atoms) by using the FLAPW-LDA+ $U$  method [7] with many types of lattice distortions. Then we have found solutions for an insulator only in  $PrRu_4P_{12}$  with the space group  $Pm\bar{3}$  ( $T_h^1$ , #200), in which P atoms are distorted by about 5 % of a lattice constant with  $\Gamma_1$  mode [8]. The result shows that the distortion coupled with anti-quadrupolar ordering of Pr  $4f^2$  states, which is discussed with  $T$  displacements [9], is not necessary for the M-I transition of  $PrRu_4P_{12}$ . The M-I transition is caused by the perfect 3 dimensional nesting of the Fermi surface consisting of the  $P_{12}$  molecular orbital with the symmetry  $xyz$ , which is the only one Fermi surface in the mother structure of  $PrRu_4P_{12}$  [10].

[1] C. Sekine *et al.*: Phys. Rev. Lett. **79** (1997) 3218.

[2] H. Sato *et al.*: Phys. Rev. B **62** (2000) 15125.

[3] H. Sugawara *et al.*: J. Magn. Magn. Mater. **226-230** (2001) 48.

[4] H. Sugawara *et al.*: J. Phys. Soc. Jpn. **69** (2000) 2938.

[5] C.H. Lee *et al.*: J. Phys.: Condens. Matter **13** (2001) L45.

[6] K. Iwasa *et al.*: Physica B in press (Proceedings of SCES2001, Ann Arbor).

[7] H. Harima: J. Magn. Magn. Mater. **226-230** (2001) 83.

[8] S.H. Curnoe *et al.*: J. Phys. Chem. Solid in press (Proceedings of ISSP-Kashiwa2001, Kashiwa).

[9] S.H. Curnoe *et al.*: Physica B in press (Proceedings of SCES2001, Ann Arbor), H. Harima *et al.*: J. Phys. Soc. Jpn Supplement in press (Proceedings of ORBITAL2001, Sendai).

[10] H. Harima and K. Takegahara: Physica B in press (Proceedings of SCES2001, Ann Arbor).



## 11. Fermi surface of magnetic uranium compounds in relativistic spin-polarized band theory

Hiroshi Yamagami

Faculty of Science, Kyoto Sangyo University, Kyoto, 603-8555, Japan

In uranium compounds the  $5f$  electrons of the uranium atom show a tendency to overlap the valence electrons of the surrounding atoms. The hybridized  $5f$ -band structure appears around the Fermi level, thus forming the  $5f$ -rich Fermi surfaces. The de Haas-van Alphen (dHvA) measurements clarify the topology of the Fermi surface as well as the effective cyclotron mass. In the magnets the  $5f$  electrons, occupied below the Fermi level, are obviously sources of magnetism and the value of magnetic moment at the uranium site is measured from the neutron scattering experiment. An essential point to study the  $5f$  electrons of magnetic uranium compounds with a band theory is how we obtain a unified understanding of  $5f$  bands just at the Fermi level and the spin-polarized  $5f$  states below the Fermi level.

As well-known the  $5f$  states are strongly affected by relativistic effects. For the spin-ordered systems an internal magnetic field couples two  $5f$ -electron states due to the spin-orbit splitting in the relativistic spin-density-functional theory (RSDFT) [1]. The coupling yields an anomalous Zeeman effect for the magnetic properties [2]. For the magnetic uranium compounds the local orbital moment thus produced is larger than the spin moment in magnitude while their moments are in opposite directions according to the third Hund's rule.

As a relativistic spin-polarized band theory including such the coupling an all-electron relativistic spin-polarized LAPW (RSPLAPW) method [3] is used to obtain a self-consistent band structure of some interesting magnetic uranium compounds. The RSPLAPW method is based on the spin-polarized coupled Dirac equation derived from the RSDFT. The magnetic configurations are considered by an application of a noncollinear technique [4]. The spin polarization effect is incorporated by the exchange-correlation potentials in a local density approximation [5]. The densities and potentials are constructed in the muffin-tin approximation.

The band structure, density of states, Fermi surface and the magnetic moments of the magnetic uranium compounds (UPdAl<sub>3</sub>, USb<sub>2</sub>, UAs<sub>2</sub>, UGe<sub>2</sub>, UNiGa<sub>5</sub>, UPtGa<sub>5</sub> etc.) obtained from the RSPLAPW band calculations are reviewed in a standpoint of the  $5f$  itinerant magnetism together with the comparison of the experimental data from the photoemission, specific heat, dHvA and neutron scattering measurements.

### References

- [1] A.K. Rajagopal and J. Callaway, *Phys. Rev.* **B7**, 1912 (1973).
- [2] H. Yamagami, A. Mavromaras, and J. Kübler, *J. Phys.:Condens. Matter* **9**, 10881 (1997).
- [3] H. Yamagami, *J. Phys. Soc. Jpn.* **67**, 3176 (1998).
- [4] H. Yamagami, *Phys. Rev.* **B61**, 6246 (2000).
- [5] U. von Barth and L. Hedin, *J. Phys. C* **5**, 1629 (1972).

## 12. Density Functional Approach with an Explicitly Orbital-Dependent Exchange and Correlation Energy Functional

M. Higuchi

*Department of Physics, Faculty of Science, Tohoku University, Sendai 980-8578, Japan*

According to the density functional theory, the ground-state electronic properties of the system can be uniquely determined by the electron density which is given by solving the so-called Kohn-Sham (KS) single-particle equation. The exchange-correlation energy functional involved in the KS equation plays a substantial role on the accuracy of the electronic structures. It is usually treated within the local-density approximation (LDA). The LDA has been successful in describing the ground-states of many systems beyond one's expectations, while some outstanding problems remain unsolved actually. The electronic structure of the strongly-correlated electron system is a typical example of these problems. Originally, the exchange and correlation energies have to be calculated by using single-particle orbitals and spectra explicitly. On the basis of this conception, Gross and co-workers have developed the optimized effective potential (OEP) method as a sophisticated scheme beyond the LDA. [1]

We have recently proposed a new expression for the explicitly orbital-dependent correlation energy functional along the OEP method.[2] It is analogous to the second-order perturbation terms where one of the Coulomb potentials is replaced with the effective potential which includes the long-, intermediate- and short-range correlations. The knowledge of the effective potential is borrowed from the homogeneous electron liquid. The validity of the effective potential is confirmed by the physically sound behaviors of the coupling-constant-averaged pair correlation function and static form factor and by the reproducibility of the correlation energy within the accuracy of 0.7 mRyd. It is also shown that the correlation between spin-parallel electrons can not be ignored quantitatively at the metallic densities. It implies that the magnitude of the Coulomb hole is not negligible as compared with that of the Fermi hole. The present correlation energy functional encourages the hybridization between the different types of orbitals in the vicinity of the Fermi level to acquire energy gains of the electron correlations.

[1] T. Grabo, T. Kreibich, S. Kurth and E. K. U. Gross, in *Strong Coulomb Correlations in Electronic Structure: Beyond the Local Density Approximation*, ed. by V. I. Anisimov (Gordon & Breach, Tokyo, 1998) Chap.4, 203.

[2] H. Yasuhara and M. Higuchi, *Phys. Rev. B* **64**, 233108 (2001).

### 13. Electronic structure and the Fermi surface of UFeGa<sub>5</sub>

T. Maehira, M. Higuchi<sup>1</sup>, A. Hasegawa<sup>2</sup>

Advanced Science Research Center, Japan Atomic Energy Research Institute, Ibaraki 319-1195, Japan

<sup>1</sup>Graduate School of Science, Tohoku University, Miyagi 980-8571, Japan

<sup>2</sup>Faculty of Science, Niigata University, Niigata 950-2181, Japan

UFeGa<sub>5</sub> with the HoCoGa<sub>5</sub>-type tetragonal crystal structure belongs to the Pauli-paramagnetic heavy electron materials. The low-temperature electronic specific heat coefficient is observed that  $\gamma_{\text{exp}} = 40 \text{ mJ/K}^2 \text{ mol}$ [1]. In this paper the energy band structure and the Fermi surface for UFeGa<sub>5</sub> are calculated by the relativistic linear augmented-plane-wave method. The exchange and correlation interactions are treated within the local density approximation (LDA). The spatial shape of the one-electron potential is determined in the muffin-tin approximation. The self-consistent calculation is performed on the assumption that the 5f electrons in UFeGa<sub>5</sub> are itinerant.

The energy band structure calculated is shown in Fig. 1. The Fermi energy  $E_F$  is located at 0.4558 Ryd. Narrow bands, which lie just above  $E_F$  and are split into two subbands by the spin-orbit interaction, are identified as the U 5f bands. A hybridization between the U 5f state and Ga 4p state occurs in the vicinity of  $E_F$ . The calculated electronic specific-heat coefficient  $\gamma_{\text{band}}$  is 19.6 mJ/K<sup>2</sup> mol. This theoretical value is about the half of the experimental value  $\gamma_{\text{exp}}$ . The disagreement between  $\gamma_{\text{band}}$  and  $\gamma_{\text{exp}}$  should be ascribed to the effect of the electron correlation which the LDA scheme fails to take into account. The enhancement factor for the electronic specific-heat coefficient, defined by  $\lambda = \gamma_{\text{exp}} / \gamma_{\text{band}} - 1$ , is 1.04. This magnitude of  $\lambda$  is the smallest among the heavy fermion uranium compounds. UFeGa<sub>5</sub> has the odd number of electrons per primitive cell, and therefore becomes the uncompensated metal where the numbers of electrons and holes on the fermi surface are not equal to each other. The 14th and 15th bands are partially occupied by electrons, which construct the electron sheets. Note that the electron sheets look quite similar to those of CeIrIn<sub>5</sub>.

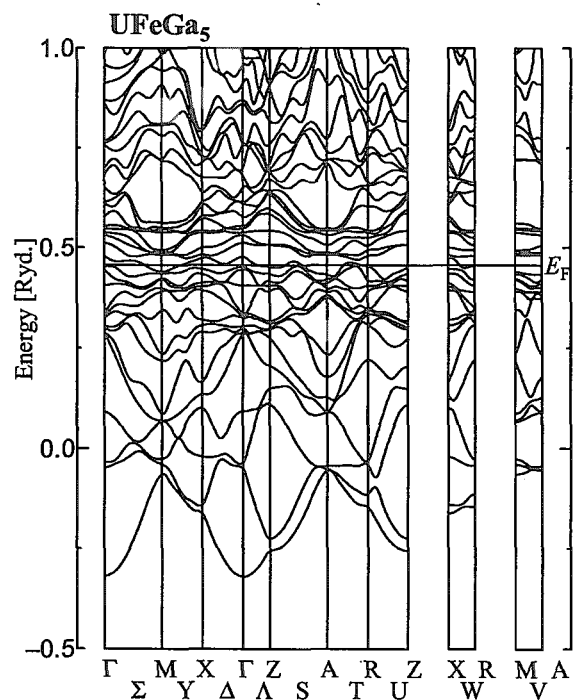


Fig. 1: Energy band structure calculated for UFeGa<sub>5</sub>.  $E_F$  shows the Fermi energy.

The origins of the de Haas-van Alphen frequency branches have been clarified satisfactorily well by our theoretical fermi surface model[2].

[1] K. Okuda and S. Noguchi: in *Physical Properties of Actinide and Rare Earth Compounds* JJAP Series 8, edited by T. Kasuya *et al.* (1993)32.

[2] Y. Tokiwa *et al.*: *J. Phys. Soc. Jpn* 70(2001)2982.

## 14. NMR Studies of magnetism and unconventional superconductivity in CeMIn<sub>5</sub>

Y. Kitaoka

*Department of Physical Science, Graduate School of Engineering Science, Osaka University, Toyonaka, Osaka 560-8531*

We report the novel interplay between the magnetism and the superconductivity in CeMIn<sub>5</sub> that forms in a tetragonal structure, focusing on spin dynamics probed by In-NQR measurement via the nuclear spin lattice relaxation rate ( $1/T_1$ ). At the normal state of CeIrIn<sub>5</sub> ( $T_c=0.4$  K) and CeCoIn<sub>5</sub> ( $T_c=2.1$  K),  $1/T_1$  is strongly T-dependent, which indicates that both are much more itinerant than known Ce-based heavy-fermion superconductors. We find that  $1/T_1T$  follows a  $1/(T+\theta)^{3/4}$  variation with the respective  $\theta=8$  and 0.5 K. This novel feature points to anisotropic, due to a layered crystal structure, spin fluctuations near a magnetic ordering [1,2]. Remarkably, as the system approaches the magnetic critical point at  $\theta=0$ ,  $T_c$  seems to be more enhanced up to 2.1 K for CeCoIn<sub>5</sub> rather than for CeIrIn<sub>5</sub>. In the superconducting (SC) state,  $1/T_1$  follows a  $T^3$  variation without the coherence peak, suggesting unconventional superconductivity with the line-node gap.

In the itinerant helical magnet CeRhIn<sub>5</sub>, we found that the Neel temperature  $T_N$  is reduced at  $P > 1.23$  GPa with an emergent *pseudogap* behavior [3,4]. The coexistence of the magnetism and the superconductivity is found in a narrow  $P$  range of 1.63–1.75 GPa [5], followed by the onset of SC state with the line-node gap at pressures exceeding a value of  $P \sim 2.1$  GPa [3,6]. By contrast, in CeIn<sub>3</sub> that forms in a cubic structure, the localized magnetic character is robust against the application of pressure up to  $P \sim 1.9$  GPa, beyond which the system evolves into an itinerant regime in which the resistive SC phase emerges [4]. We discuss the relationship between the phase diagram and the magnetic fluctuations.

The works presented were done in collaboration with Y. Kawasaki, T. Mito, S. Kawasaki, G.-q. Zheng, D. Aoki, Y. Haga, R. Settai, Y. Onuki.

- [1] G.-q. Zheng *et al.*, Phys. Rev. Lett. 86, 4664 (2001).
- [2] Y. Kawasaki *et al.*, unpublished.
- [3] T. Mito *et al.*, Phys. Rev. B 63, 220507(R) (2001).
- [4] S. Kawasaki *et al.*, to appear in Phys. Rev. B in January, 2002.
- [5] T. Mito *et al.*, unpublished.
- [6] Y. Kohori *et al.*, Euro. Phys. J. 18, 601 (2000).

## 15. Spin Fluctuation Induced Superconductivity Controlled by Orbital Fluctuation

Tetsuya Takimoto<sup>a</sup>, Takahiro Maehira<sup>a</sup>, Takashi Hotta<sup>a</sup>, and Kazuo Ueda<sup>b,a</sup>

<sup>a</sup>Advanced Science Research Center, Japan Atomic Energy Research Institute, Tokai, Ibaraki 319-1195, Japan

<sup>b</sup>ISSP, University of Tokyo, 5-1-5 Kashiwanoha, Kashiwa, Chiba 277-8581, Japan

Since the discovery of superconductivity in  $\text{CeCu}_2\text{Si}_2$ , intensive investigations have been made to clarify the mechanism of heavy-fermion superconductivity. Especially, due to the experimental results for recently discovered Ce-based heavy fermion superconductors  $\text{CeTIn}_5$  ( $T=\text{Rh, Ir, and Co}$ ), much more attentions have been focussed on unconventional superconductivity in  $f$ -electron systems. From the theoretical viewpoint, the phenomenological approach has been mainly developed due to the complexity of  $f$ -electron systems. Thus, it is important to address superconductivity microscopically based on a simple model Hamiltonian.

In order to describe the band structure of quasi-particles around the Fermi level, first the tight-binding model is constructed by considering only the  $f$ -electron hopping between neighboring Ce ions. Note that due to the large spin-orbit coupling, it should be enough to take into account only the sextuplet of  $j=5/2$ , where  $j$  is the magnitude of the total angular momentum. Since  $\Gamma_8$  states is expected to be lower than  $\Gamma_7$  by taking into account the arrangement of anions surrounding Ce ion of  $\text{CeTIn}_5$ , it will be minimal to address the  $\Gamma_8$  states only in order to investigate the low temperature physics. By further adding the on-site Coulomb interaction between  $f$ -electrons and the tetragonal CEF term, a new simple Hamiltonian is proposed to investigate properties of heavy fermion systems at low temperatures. Based on this Hamiltonian, we study the superconducting transition for respective irreducible representation within RPA. When the tetragonal CEF splitting  $\varepsilon$  is small, cancellation between spin and orbital fluctuations destabilizes  $d_{x^2-y^2}$ -wave superconductivity. With increasing the tetragonal CEF energy splitting,  $d_{x^2-y^2}$ -wave superconductivity mediated by antiferromagnetic spin fluctuations emerges out of the suppression of orbital fluctuations. We argue that the present scenario can be applied to recently discovered superconductors  $\text{CeTIn}_5$ .

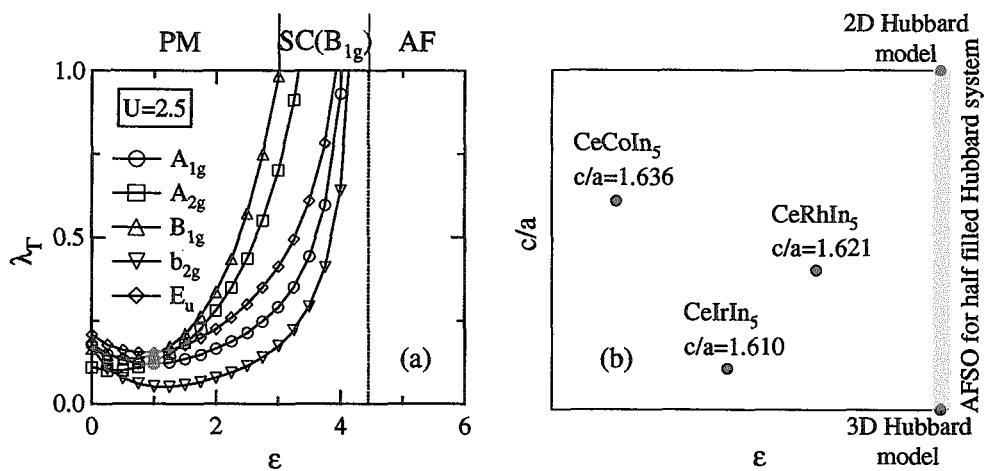


Figure 1: (a) Maximum eigenvalue vs.  $\varepsilon$  for the respective irreducible representation at  $U=U'=2.5$  where  $\varepsilon$  denotes the tetragonal CEF splitting energy between  $\Gamma_8$ -states. (b) Schematic plot  $c/a$  vs.  $\varepsilon$  to illustrate a comparison between our theory and actual  $\text{CeTIn}_5$  compounds where  $c/a$  is the ratio between lattice constants.

## 16. Superconductivity in CeMIn<sub>5</sub> and Related Compounds

J. D. Thompson, W. Bao, A. Bianchi, F. Bouquet<sup>‡</sup>, N. Curro, R. A. Fisher<sup>‡</sup>, Z. Fisk, R. Goodrich<sup>†</sup>, D. Hall<sup>†</sup>, A. Llobet-Megias, L. Morales, N. Moreno-Salazar, R. Movshovich, T. Murphy<sup>†</sup>, M. Nicklas, P. G. Pagliuso, N. E. Phillips<sup>‡</sup>, J. L. Sarrao, V. Sidorov

Los Alamos National Laboratory; <sup>†</sup>U. C. Berkeley; <sup>‡</sup>Louisiana State University; <sup>†</sup>NHMFL, Florida State University

Members of the CeMIn<sub>5</sub> family are unconventional heavy-fermion superconductors at atmospheric pressure (M=Co and Ir) or at modest pressures (M=Rh). Their layered crystal structure and anisotropy in their electronic and magnetic properties appear to play a role in producing relatively high superconducting transition temperatures, which for M=Co and Rh exceed 2K. Each member presents some unusual property associated with superconductivity: the pressure-induced transition from antiferromagnetic to superconducting states in CeRhIn<sub>5</sub> is weakly first-order; superconductivity in CeCoIn<sub>5</sub> appears to develop in proximity to a quantum-critical point, and under some circumstances, the field-induced normal/superconducting transition is first order; and the transition to a zero-resistance state in CeIrIn<sub>5</sub> occurs at a temperature three times higher than the bulk superconducting transition. Relationships between these properties are beginning to emerge from alloying and high pressure studies. Ce<sub>2</sub>RhIn<sub>8</sub> and Ce<sub>2</sub>IrIn<sub>8</sub> are two-layer variants of the single-layer 115 members. Like CeRhIn<sub>5</sub>, Ce<sub>2</sub>RhIn<sub>8</sub> also is an antiferromagnet at atmospheric pressure and becomes a bulk superconductor with applied pressure. As will be discussed, in some respects Ce<sub>2</sub>RhIn<sub>8</sub> appears to be a dimensional hybrid of CeRhIn<sub>5</sub> and the infinite layer member CeIn<sub>3</sub>.

Analogies between these Ce-based materials and the cuprates suggests that an approach to raising the superconducting transition temperature is to increase the characteristic spin-fluctuation temperature, as might be accomplished, for instance, by replacing Ce with a 3d- or 5f-electron element. Initial exploration shows that single-crystal PuCoGa<sub>5</sub> is a bulk superconductor below 18.5 K, nearly an order of magnitude higher T<sub>c</sub> than in the Ce compounds. Further experiments will be required to determine if the superconductivity is unconventional and if PuCoGa<sub>5</sub> is a heavy-fermion system.

## 17. Superconducting Gap Structure of Heavy-Fermion superconductor CeCoIn<sub>5</sub>

Koichi Izawa, Hidemasa Yamaguchi, Yuji Matsuda,  
Hiroaki Shishido<sup>1</sup>, Rikio Settai<sup>1</sup> and Yoshichika Onuki<sup>1</sup>

*Institute for Solid State Physics, University of Tokyo*

<sup>1</sup>*Graduate School of Science, Osaka University*

The superconducting gap structure, especially the direction of the nodes, is an unsolved issue in most of unconventional superconductors. Since the superconducting gap structure is closely related with the pairing interaction, its determination is crucial for understanding the mechanism of superconductivity. Recently it is pointed out that the thermal conductivity is a powerful tool for probing the gap structure. Here, to clarify the gap structure of heavy-fermion superconductor CeCoIn<sub>5</sub>, the in-plane thermal conductivity has been measured in magnetic field  $H$  rotating within the 2D superconducting plane. As shown in fig.1, clear twofold and fourfold terms are found in the angular dependence of the thermal conductivity  $\kappa(\theta, H)$ , where  $\theta = (\mathbf{H}, \mathbf{q})$  and  $\mathbf{q}$  is thermal current. The twofold term which has a minimum at  $\mathbf{H} \perp \mathbf{q}$  appears as a result of the difference of the effective DOS for the quasiparticles traveling parallel to the vortex and for those moving in the perpendicular direction. On the other hand, the fourfold symmetry which is characteristic of a superconducting gap with nodes along the  $(\pm\pi, \pm\pi)$ -directions is resolved. This result shows that the symmetry of CeCoIn<sub>5</sub> most likely belongs to  $d_{x^2-y^2}$  (fig.2), implying that the anisotropic antiferromagnetic fluctuation plays an important role for the superconductivity. CeCoIn<sub>5</sub> is the second example after high- $T_c$  cuprates, in which nodal structure in the plane is successfully specified.

Thermal conductivity measurement also reveals a first order phase transition (FOPT) at  $H_{c2}$ . We also discuss this FOPT.

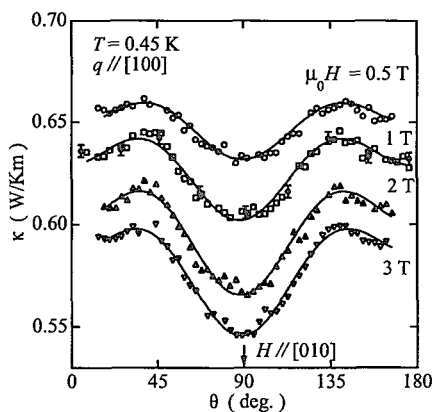


Figure 1:

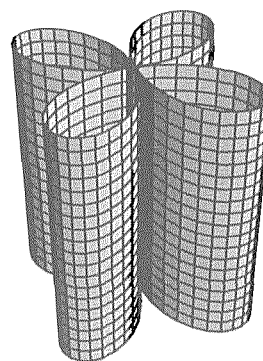


Figure 2:

## 18. Low Temperature Magnetization of CeTIn<sub>5</sub> (T=Co,Ir)

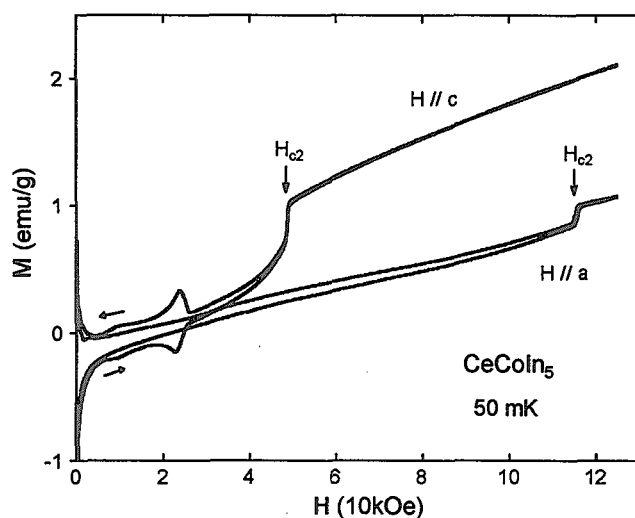
Takashi Tayama<sup>a</sup>, Akira Harita<sup>a</sup>, Toshiro Sakakibara<sup>a</sup>, Yoshinori Haga<sup>b</sup>, Hiroaki Shishido<sup>c</sup>, Rikio Settai<sup>c</sup>, and Yoshichika Onuki<sup>c</sup>

<sup>a</sup>*ISSP, University of Tokyo, 5-1-5 Kashiwanoha, Kashiwa, Chiba 277-8551*

<sup>b</sup>*Advanced Science Research Center, Japan Atomic Energy Research Institute, Tokai, Ibaraki 319-1195*

<sup>c</sup>*Graduate School of Science, Osaka University, Toyonaka, Osaka 560-0043*

We report dc magnetization results on the newly discovered heavy-fermion superconductor CeTIn<sub>5</sub> (T=Co [1], Ir [2]). In CeCoIn<sub>5</sub> ( $T_c=2.3\text{K}$ ), the isothermal magnetization curve for both a- and c-directions shows a clear magnetization jump at the upper critical field  $H_{c2}$  ( $H_{c2}^a=116\text{ kOe}$ ,  $H_{c2}^c=49\text{ kOe}$ ) below  $T_{cr}\sim 0.7\text{ K}$  ( $=0.3 T_c$ ), suggesting a strong Pauli paramagnetic suppression in the even parity pairing. No indication of the Fulde-Ferrell-Larkin-Ovchinnikov state is found. Temperature dependence of the magnetization  $M(T)$  in the normal state above  $H_{c2}$  exhibits non-Fermi-liquid behavior down to 150 mK, implying the existence of antiferromagnetic fluctuations behind the unconventional superconductivity [3]. In addition we observed an unusual peak effect for  $H//c$  in fields 5~30 kOe below 150 mK ( $=0.06T_c$ ), whose anomalous temperature dependence cannot be simply explained by ordinary mechanism. In contrast, CeIrIn<sub>5</sub> ( $T_c=0.4\text{K}$ ) show no first-order phase transition at  $H_{c2}$ , though non-Fermi liquid behavior was observed in the  $M(T)$  curve.



[1] C. Petrovic *et al.*, J. Phys.: Condens. Matter **13**, 337 (2001).

[2] C. Petrovic *et al.*, Europhys. Lett. **53**, 354 (2001).

[3] K. Izawa *et al.*, Phys. Rev. Lett. **87**, 057002 (2001).



19. Photoemission Study of  $\text{CeTIn}_5$  ( $T=\text{Rh, Ir}$ )

Shin-ichi Fujimori<sup>1</sup>, Jun Okamoto<sup>1</sup>, Kazutoshi Mamiya, Testuo Okane<sup>1</sup>, Atushi Fujimori<sup>1,2</sup>,  
Hisatomo Harima<sup>3</sup>, Dai Aoki<sup>4</sup>, Shuugo Ikeda<sup>5</sup>, Hiroaki ShiShido<sup>5</sup>, Yoshinori Haga<sup>6</sup>,  
Yoshifumi Tokiwa<sup>5,6</sup> and Yoshichika Ōuki<sup>5,6</sup>

<sup>1</sup>Synchrotron Radiation Research Center, Japan Atomic Energy Research Institute,  
SPring-8, Mikazuki, Hyogo 679-5148, Japan

<sup>2</sup>Department of Physics, Graduate School of Science, University of Tokyo, Hongo 7-3-1, Tokyo 113-0033, Japan

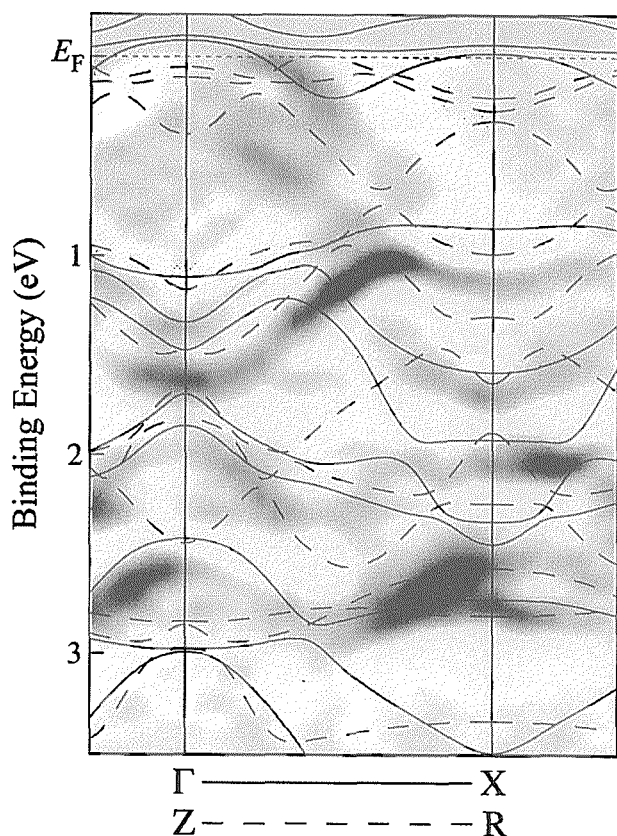
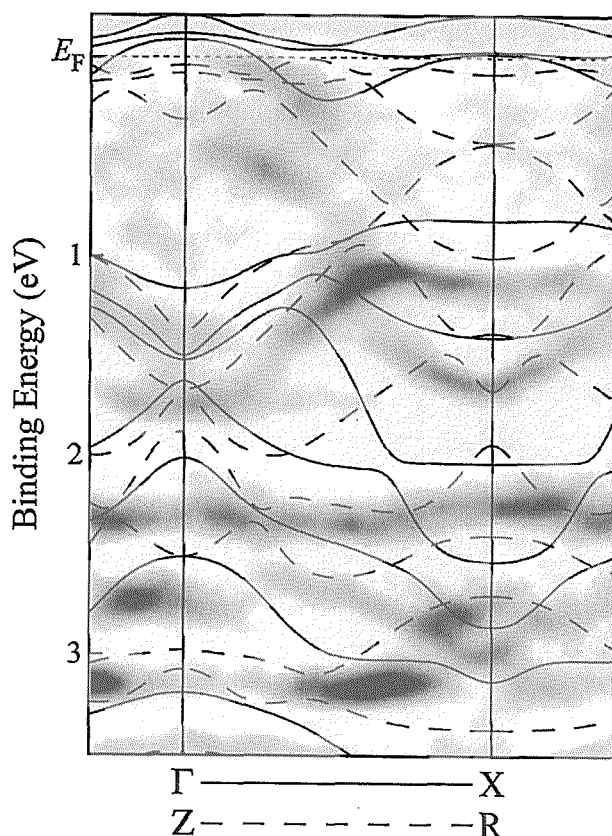
<sup>3</sup>ISIR-SANKEN, Osaka University, Ibaraki, Osaka 567-0043, Japan

<sup>4</sup>DRFMC-SPSMS, CEA, 38054, Grenoble, Cedex 9, France

<sup>5</sup>Graduate School of Science, Osaka University, Toyonaka, Osaka 560-0043, Japan

<sup>6</sup>Advanced Science Research Center, Japan Atomic Energy Research Institute, Tokai, Ibaraki 319-1195, Japan

In the present study, the electronic structures of  $\text{CeTIn}_5$  ( $T=\text{Rh, Ir}$ ) are investigated by the high-resolution angle-resolved photoelectron spectroscopy (ARPES) with He-discharged lamp, and the resonant photoelectron spectroscopy (RESPES) with synchrotron radiations from BL23SU SPring-8. The ARPES spectra were measured by He II ( $h\nu=21.2\text{eV}$ ), and the sample temperature was kept at 15K. Figures show the “band dispersions” of (a) $\text{CeRhIn}_5$  and (b) $\text{CeIrIn}_5$ , derived from their ARPES spectra, together with the results of the FLAPW band structure calculation, treating the Ce 4*f* electrons as itinerant. The dark part in the image corresponds to peak position in the experimental spectra, and solid and dashed lines correspond to the band dispersions by the calculations. The comparison of these spectra with the results of the calculation suggests that essential spectral features are well correspond to the calculated dispersion, except for the nearly flat bands located at around  $E_F$  in the calculation, which have large contributions from Ce 4*f* states. The results of the 4*d*-4*f* RESPES experiments ( $h\nu\sim 880\text{eV}$ ) showed that Ce 4*f* electrons are relatively localized in both compounds.

(a)  $\text{CeRhIn}_5$ (b)  $\text{CeIrIn}_5$ 

## 20. Analysis of superconductivity in $\text{Sr}_2\text{RuO}_4$ on the basis of the six-band Hubbard model

Shigeru Koikegami<sup>1,2</sup>, Takashi Yanagisawa<sup>2</sup> and Yoshiyuki Yoshida<sup>1,2</sup>

<sup>1</sup>Japan Science and Technology Corporation

<sup>2</sup>Nanoelectronics Research Institute, AIST Tsukuba Central 2,  
Tsukuba 305-8568

In recent years, the spin-triplet superconductor  $\text{Sr}_2\text{RuO}_4$  has been studied extensively in order to clarify the momentum dependence of its gap function. Hasegawa et al. have listed the possible odd-parity states on the basis of the group-theoretical analysis. [1] They have insisted that the effective interaction between the electrons on the non-equivalent Ru sites is crucial to stabilize the gap function with the horizontal line node. Zhitomirsky and Rice have successfully shown that this gap function may lead to the temperature dependence of the specific heat observed in experiments. [2]

Inspired by these important results, we study the quasi-two-dimensional (Q2D) six-band Hubbard model, which can well reproduce the Fermi surfaces measured by de Haas van Alphen effect. [3] Furthermore, we introduce Coulomb interactions between the electrons on the non-equivalent Ru sites. Our model is considered as an application of Kondo's two-band mechanism superconductivity to the spin-triplet Cooper pairing. [4] In our model the inter-site Hund coupling can work as the effective interaction for the spin-triplet pairing together with the band hybridization effect mediated by the inter-layer transfers. We investigate the possibility of this mechanism by mean-field theory and find that the spin-triplet superconductivity is more stable than the spin-singlet one for the realistic parameters.

## References

- [1] Y. Hasegawa *et al.* *Jour. Phys. Soc. Jpn.*, 69:336, 2000.
- [2] M. E. Zhitomirsky and T. M. Rice. *Phys. Rev. Lett.*, 87:057001, 2001.
- [3] Y. Yoshida *et al.* *Jour. Phys. Soc. Jpn.*, 68:9, 1999.
- [4] J. Kondo. *Prog. Theor. Phys.*, 29:1, 1963.

## 21. Perturbation Theory on the Superconductivity of Heavy Fermion Superconductors $\text{CeIr}_x\text{Co}_{1-x}\text{In}_5$

Department of Physics, Kyoto University  
Y.Nisikawa, H.Ikeda and K.Yamada

Workshop on "Orbital ordering and fluctuations in d- and f- electron system"  
2002.3.6(Poster)

We reformulate the Éliashberg's equation for the superconducting transition within the quasi-particle description, which takes account of the heavy electron mass. We discuss the superconductivity of  $\text{CeIr}_x\text{Co}_{1-x}\text{In}_5$  by using such a renormalized formula. On the basis of an effective two-dimensional Hubbard model which represents the most heavy quasi-two dimensional Fermi surface with  $f$ -character of  $\text{CeIr}_x\text{Co}_{1-x}\text{In}_5$ , both normal and anomalous self-energies are calculated up to third order with respect to the renormalized on-site repulsion  $U$  between quasi-particles. The superconducting transition temperature is obtained by solving the Éliashberg's equation. Reasonable transition temperatures are obtained for moderately large  $U$ . It is found that the momentum and frequency dependence of spin fluctuations given by RPA-like terms gives rise to the d-wave pairing state, while the vertex correction terms are important for obtaining reasonable transition temperatures and for differentiating  $n$ -dependence of  $T_c$ . These obtained results seem to explain the  $x$ -dependence of  $T_c$  in  $\text{CeIr}_x\text{Co}_{1-x}\text{In}_5$  and confirm the usefulness of the perturbation theory with respect to  $U$ .

## 22. Kondo hole in one-dimensional Kondo insulators

Isao Maruyama<sup>A</sup>, Naokazu Shibata<sup>B</sup> and Kazuo Ueda<sup>A,C</sup>

Institute for Solid State Physics<sup>A</sup>,  
Department of Basic Science, University of Tokyo<sup>B</sup>,  
Japan Atomic Energy Research Institute<sup>C</sup>

A Kondo hole, depletion of a localized spin, in the Kondo lattice model describes the substitution of a non-magnetic impurity into heavy fermion systems. To investigate properties of a Kondo hole in Kondo insulators we consider a Kondo hole in the half-filling one-dimensional Kondo lattice model which has a spin gap and a charge gap. To study the condition for formation of localized moments we consider the potential  $\epsilon$  and the on-site Coulomb term  $U$  on the impurity site  $n_d$ .

$$\begin{aligned}
 H = & \sum_{\langle n,n' \rangle, s} t_{n,n'} c_{ns}^\dagger c_{n's} + J \sum_{n \neq n_d} \mathbf{S}_n \cdot \mathbf{s}_n \\
 & + \epsilon \sum_s c_{n_d s}^\dagger c_{n_d s} + U c_{n_d \uparrow}^\dagger c_{n_d \uparrow} c_{n_d \downarrow}^\dagger c_{n_d \downarrow}
 \end{aligned} \tag{1}$$

The ground state phase diagram is obtained by using the Lanczos method. We can determine the ground state phase diagram of infinite system size from the alternating system size dependence of the phase boundaries determined by the Lanczos method. Impurity susceptibilities as a function of temperature are obtained by the finite temperature density-matrix renormalization group for systems with an impurity. The ground state phase diagram is consistent with the behavior of impurity susceptibilities at low temperatures.

A remarkable feature of the ground state phase diagram in the  $(U, \epsilon)$  plane is that there is a region where magnetic state is stable and furthermore the magnetic state extends to the region of negative  $U$  more for smaller  $J$ . In fact, this result is confirmed by the  $t/J$  perturbation from the strong coupling limit. This perturbation result means that the magnetic state becomes stable because of hopping processes.

Concerning the nature of the magnetic moment, various impurity susceptibilities at low temperatures show that the magnetic moment is localized around the impurity site but spreads into surrounding Kondo lattices more for smaller  $J$ . This trend can be understood from the spin gap of the Kondo insulator, which becomes smaller for smaller  $J$ . This spatial spreading of the magnetic moment is the key to understand the extension of the magnetic region, because the spreaded magnetic moment feels effectively weaker Coulomb repulsion or attraction which exists only on the impurity site.

23. Heavy Fermion Behavior and Orbital Fluctuations in  $\text{LiV}_2\text{O}_4$ 

Yasufumi Yamashita<sup>1</sup> and Kazuo Ueda<sup>1,2</sup>  
 Institute for Solid State Physics, University of Tokyo<sup>1</sup>,  
 Japan Atomic Energy Research Institute<sup>2</sup>

The metallic spinel compound  $\text{LiV}_2\text{O}_4$  is known to show heavy fermion behaviors (for example,  $\gamma \sim 350\text{J/mol}\cdot\text{K}$ ), but its mechanism is still unknown. In general, a highly frustrated lattice structure of  $\text{LiV}_2\text{O}_4$  is expected to suppress any kind of long-range order (LRO). Therefore, the effects of orbital fluctuations are one of the possible candidates to explain the formation of the heavy-mass quasi-particle. We have examined the role of orbital fluctuations in  $\text{LiV}_2\text{O}_4$ , starting from the quarter-filled  $t_{2g}$ -band Hubbard model on a pyrochlore lattice.

In order to describe many-body correlations of the  $t_{2g}$  electrons, we introduce the 35 generators of the  $\text{SU}(6)$  group. These generators consist of the pure spin degrees of freedom ( $\text{SU}(2)$  Pauli matrices), the pure orbital ( $\text{SU}(3)$  Gell-Mann matrices), and the coupled modes of the two ( $\text{SU}(2) \times \text{SU}(3)$  matrices). First of all, we numerically calculated the susceptibility of the non-interacting  $t_{2g}$  electrons on a pyrochlore lattice with nearest neighbor hoppings. As a result, all thirty-five components of fluctuations are found to have the same order of magnitudes. Accordingly we expect enhancement for free energy about 35/3 times larger, supposing that orbital fluctuations survive due to the suppression of LRO by the geometrical frustration.

Next we evaluate the effect of the coulomb interactions by using the RPA approximation. For simplicity we take the  $\text{SU}(6)$  limit of  $U = U'$  and  $J = 0$ , where the interactions are represented by the unique  $\text{SU}(6)$  invariant form. Since we are primarily interested in the mass enhancement in the electronic specific heat coefficient, we calculate the imaginary part of the susceptibility for  $\omega \ll 1$  to obtain its  $\omega$ -linear dependence. By solving the RPA equations, we find that only the charge fluctuations are suppressed, while the others are enhanced with increasing  $U$ . The developments of the orbital-related 32 fluctuations lead to plenty of mass enhancement under a critical value of  $U$ . From these facts, we conclude that the heavy fermion behaviors observed in  $\text{LiV}_2\text{O}_4$  has its origin in the frustrated lattice structure and the enhanced spin, orbital, and coupled modes fluctuations.

## 24. Spin-Peierls transition in $S = 1$ antiferromagnetic Heisenberg chain with spin-phonon coupling

Hiroaki Onishi and Seiji Miyashita<sup>1</sup>

*Department of Earth and Space Science, Graduate School of Science, Osaka University, 1-1 Machikaneyama-cho, Toyonaka, Osaka 560-0043*

<sup>1</sup>*Department of Applied Physics, Graduate School of Engineering, University of Tokyo, 7-3-1 Hongo, Bunkyo-ku, Tokyo 113-8656*

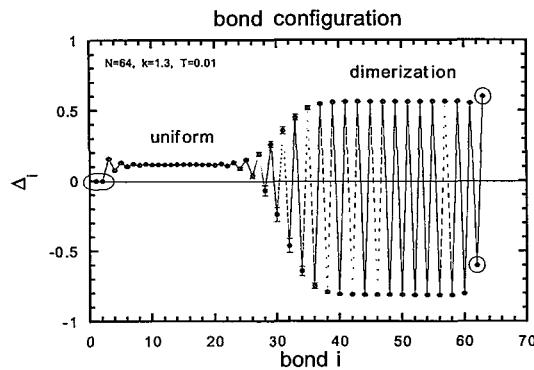
The spin-Peierls system shows multiple phenomena of spin and lattice degrees of freedom due to a spin-phonon coupling. We investigate a one-dimensional antiferromagnetic Heisenberg model coupled to a lattice distortion as a spin-Peierls system. Hamiltonian is given by

$$H = J \sum_{i=1}^N (1 + \Delta_i) \mathbf{S}_i \cdot \mathbf{S}_{i+1} + \frac{k}{2} \sum_{i=1}^N \Delta_i^2,$$

where the distortion of the exchange coupling is assumed to be proportional to the lattice distortion. For  $S = 1/2$ , the lattice dimerizes as  $\Delta_i = (-1)^i \delta$  for any value of  $k$  in the ground state.

We study the case of  $S = 1$  by a quantum Monte Carlo method [1] instead of  $S = 1/2$ . The chain has the instability to a dimerized chain only for small values of  $k$ , unlike the case of  $S = 1/2$ . In the ground state, the spin state is either the Haldane state or the dimer state according to the degree of bond dimerization. The spin state is found to be the dimer state whenever the lattice distorts spontaneously due to the spin-phonon coupling. We find that the first-order transition occurs between the uniform Haldane state and the dimerized state at a critical value of  $k$ . Consequently, two non-magnetic states coexist in the chain. We investigate microscopic structures of spin and lattice in the coexistent state. We obtain a soliton structure of the domain wall between the uniform Haldane state and the dimerized state as shown in the figure below.

When we assumed that the whole chain takes the simple dimerized configuration,  $\Delta_i = (-1)^i \delta$ , the bond configuration is characterized by one parameter  $\delta$ . In the coexistent state of two bond configurations, however, we find an asymmetrical bond alternation  $\Delta_i \neq -\Delta_{i+1}$  in the dimerized region. We carry out a variational calculation with respect to extended parameters in the coexistent state and confirm that the asymmetrical configuration appears intrinsically in the coexistent state.



[1] H. Onishi and S. Miyashita: Phys. Rev. B 64 (2001) 014405.

## 25. Magnetic Properties of UNiGa<sub>5</sub> and UPtGa<sub>5</sub>

Y. Tokiwa<sup>1,2</sup>, Y. Haga<sup>1</sup>, N. Metoki<sup>1</sup>, Y. Ishii<sup>1</sup>, and Y. Onuki<sup>1,2</sup>

<sup>1</sup>Advanced Science Research Center, Japan Atomic Energy Research Institute, Tokai, Naka, Ibaraki 319-1195

<sup>2</sup>Graduate School of Science, Osaka University, Toyonaka, Osaka 560-0043

The crystal and magnetic structures of  $5f$  itinerant antiferromagnets UNiGa<sub>5</sub> and UPtGa<sub>5</sub> were studied by means of neutron scattering. Figure 1 shows  $(h,h,h)$  scan in UNiGa<sub>5</sub>. We observed clear antiferromagnetic reflections at  $(1/2, 1/2, 1/2)$  and  $(3/2, 3/2, 3/2)$ . The antiferromagnetic peaks were observed at the magnetic Bragg points with half-integer reflection indices. This data indicate that the antiferromagnetic propagation vector in UNiGa<sub>5</sub> is  $[1/2, 1/2, 1/2]$ . The magnetic moment in UNiGa<sub>5</sub> was estimated to be a relatively large moment of  $0.9 \mu_B/U$  along the  $[0,0,1]$  direction. On the other hand,  $(1,0,1/2)$  and  $(1,0,3/2)$  magnetic reflections were observed in UPtGa<sub>5</sub>, as shown in Fig. 2. We observed antiferromagnetic reflections at  $(h,k,1/2)$ . These magnetic Bragg peaks clearly show that the antiferromagnetic propagation vector  $Q$  is  $[0,0,1/2]$ . An ordered moment is  $0.24 \mu_B/U$  along  $[0,0,1]$  direction. The remarkable difference in magnetic structure and the moment size is discussed in terms of the strength of the hybridization between U- $5f$  and Ga- $4p$  band, controlled by the atomic position  $z$  of Ga 4i site.

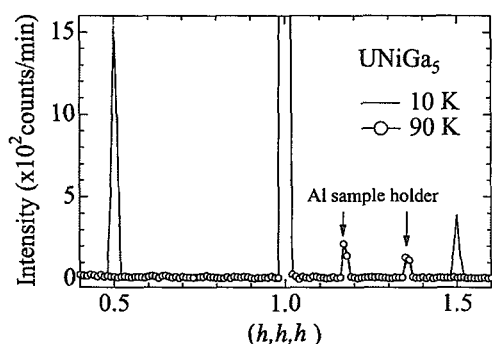


Fig.1  $(h,h,h)$  scan in UNiGa<sub>5</sub>

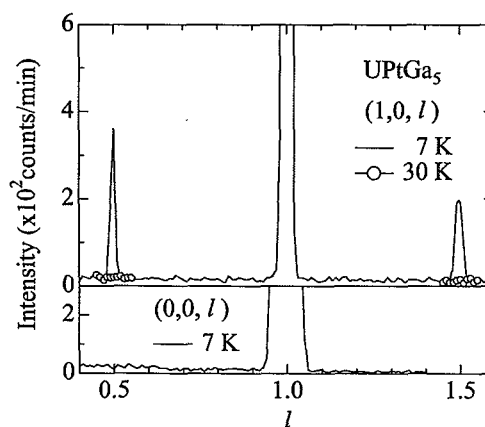


Fig.2  $(1,0,l)$  and  $(0,0,l)$  scans in UNiGa<sub>5</sub>

## 26. Ga NMR/NQR study of $UTGa_5$ ( $T = Pt, Ni$ )

Harukazu Kato<sup>A</sup>, Hironori Sakai<sup>A</sup>, Yoshihumi Tokiwa<sup>A,B</sup>, Yoshichika Ōuki<sup>A,B</sup>, Shinsaku Kambe<sup>A</sup>, and Russell E. Walstedt<sup>A</sup>

<sup>A</sup> *Advanced Science Research Center, Japan Atomic Energy Research Institute*

<sup>B</sup> *Dept. of Science, Osaka University*

In recent years, unconventional superconductivity has been found in  $CeTIn_5$  ( $T = Co, Rh, In$ ). In this context, magnetic properties of the same type of uranium compounds have attracted much interest. There is a large family of  $UTGa_5$  compounds ( $T$ : Transition metal), which crystallizes in the  $HoCoGa_5$ -type structure shown in Fig.1. It can be regarded as the alternating layers of  $UGa_3$  and  $TGa_2$ , which are stacked sequentially along the  $c$  axis. There are two crystallographically inequivalent Ga sites, namely, Ga(1) at  $(1/2, 1/2, 0)$  and Ga(2) at  $(1/2, 0, z)$ . The T atom has only one crystallographic site.

In this family,  $UPtGa_5$  and  $UNiGa_5$  are 5*f*-itinerant antiferromagnets with Neel temperature  $T_N = 26$  K (Pt), 86 K (Ni) and an electronic specific coefficient  $\gamma = 57$  mJ/mol  $K^2$  (Pt), 30 mJ/mol  $K^2$  (Ni). Remarkably, recent neutron scattering experiments reveal that  $UPtGa_5$  and  $UNiGa_5$  are quite different in magnetic structure below  $T_N$ . From the viewpoint of electronic structure, the difference in magnetic structure is somewhat surprising, since the two compounds show almost identical Fermi surface properties in the paramagnetic state. To elucidate the magnetism of  $UTGa_5$ , at first, we performed <sup>69,71</sup>Ga-NMR/NQR studies for  $UPtGa_5$ .

From the NMR spectrum in the paramagnetic temperature region, we obtain values for the splitting parameter  $\nu_Q$  and the asymmetry parameter  $\eta$ , which characterize the electrical field gradients at the nuclear sites, for Ga(1) and Ga(2). The hyperfine coupling constants  $A_{hf}^{para}$  in the paramagnetic state have also been evaluated. Figure 2 shows the zero-applied-field NMR spectrum in the antiferromagnetic temperature region. The spectrum can be satisfactorily explained as resonances of Ga(1) and Ga(2), which reflect Zeeman interaction with transferred hyperfine fields, in addition to the electric quadrupole interaction. For Ga(2), the magnitude of the transferred field has been evaluated from the spectrum, yielding a value for the hyperfine coupling constant  $A_{hf}^{AF}$  in the antiferromagnetic state. The estimated value of  $A_{hf}^{AF}$  is an order of magnitude larger than that of  $A_{hf}^{para}$ . This implies the existence of a strong hyperfine interaction path through the  $PtGa_2$  layer. The mechanism of the hyperfine interaction will be discussed in terms of RKKY interactions.

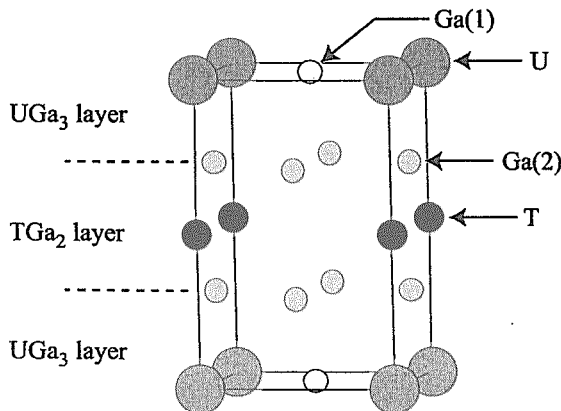


Fig. 1 Crystal structure of  $UTGa_5$

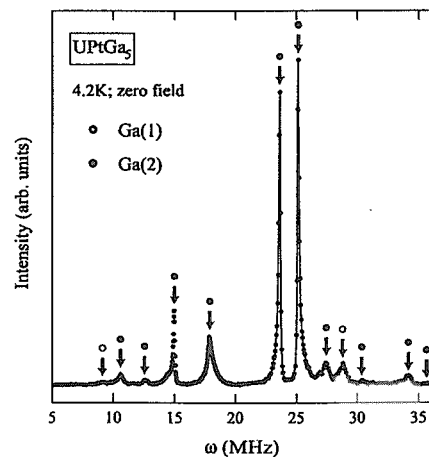


Fig. 2 zero-applied-field NMR spectrum of  $UPtGa_5$



## 27. Superconductivity in a pyrochlore oxide $\text{Cd}_2\text{Re}_2\text{O}_7$

H. Sakai<sup>1,2</sup>, H. Kato<sup>1</sup>, S. Kambe<sup>1</sup>, R. E. Walstedt<sup>1</sup>  
H. Ohno<sup>2</sup>, M. Kato<sup>2</sup>, K. Yoshimura<sup>2</sup> and H. Matsuhata<sup>3</sup>

<sup>1</sup>Advanced Science Research Center, Japan Atomic Energy Research Institute, Tokai, Ibaraki 319-1195, JAPAN

<sup>2</sup>Department of Chemistry, Graduate School of Science, Kyoto University, Kyoto 606-8502, JAPAN

<sup>3</sup>Division of Electronics, National Institute of Advanced Industrial Science and Technology, Tsukuba, Ibaraki 305-8568

Recently the pyrochlore oxide  $\text{Cd}_2\text{Re}_2\text{O}_7$  has been found to exhibit superconductivity at 1.1 K [1, 2]. The upper critical field  $H_{c2}$  extrapolated to 0 K is estimated to be about 0.8 T, using the resistivity measurements under applied field. The plot of  $H_{c2}$  vs  $T$  indicates that the Cooper pairs are composed of rather heavy quasiparticles. The structural phase transition at  $T^* \sim 200$  K in  $\text{Cd}_2\text{Re}_2\text{O}_7$  has been investigated by using X-ray and electron diffraction experiments and  $^{111}\text{Cd}$  NMR measurements. The susceptibility for  $\text{Cd}_2\text{Re}_2\text{O}_7$  in the high temperature region ( $T > 400$  K  $\gg T^*$ ) obeys the Curie-Weiss law with a large and negative Weiss temperature ( $\Theta \sim -1500$  K), which leads to the antiferromagnetic exchange interaction with a large geometrical spin frustration. Studies of X-ray and electron diffraction measurements suggests the tetramerization of Re below  $T^*$ , which induces a nano-sized striped structure. From  $^{111}\text{Cd}$  NMR experiments, the decrease of total susceptibility corresponds to the decrease of spin susceptibility below  $T^*$ , and a large orbital susceptibility is observed below  $T^*$  based on the  $K-\chi$  plot. The transferred hyperfine coupling constant slightly varies through  $T^*$ . The spin-lattice relaxation rate  $1/T_1$  suggests the presence of a pseudo-energy-gap. These results suggest a pseudogap state below  $T^*$  from the analogy of the high- $T_c$  copper oxides. These results may be concerned with the origin of superconductivity in this system [3].

[1] H. Sakai, K. Yoshimura, H. Ohno, H. Kato, S. Kambe, R. E. Walstedt, T. D. Matsuda, Y. Haga and Y. Onuki, *J. Phys.:Condens. Matter* **13**, L785 (2001).

[2] M. Hanawa, Y. Muraoka, T. Tayama, T. Sakakibara, J. Yamaura and Z. Hiroi, *Phys. Rev. Lett.* **87**, 187001 (2001).

[3] H. Sakai, H. Ohno, M. Kato, K. Yoshimura, S. Kambe, R. E. Walstedt and H. Matsuhata, in preparation.

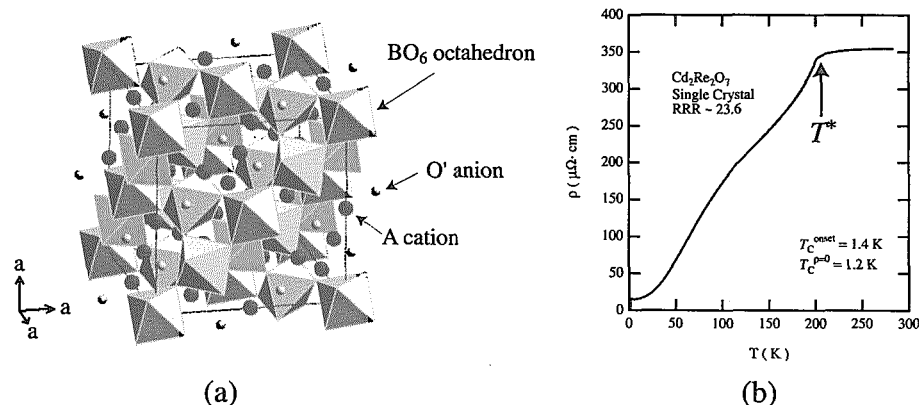


Figure 1: (a) Crystal structure of a pyrochlore oxide  $\text{A}_2\text{B}_2\text{O}_7$  (b) Temperature dependence of resistivity for  $\text{Cd}_2\text{Re}_2\text{O}_7$

This is a blank page.

# 国際単位系 (SI) と換算表

表1 SI基本単位および補助単位

量	名称	記号
長さ	メートル	m
質量	キログラム	kg
時間	秒	s
電流	アンペア	A
熱力学温度	ケルビン	K
物質質量	モル	mol
光度	カンデラ	cd
平面角	ラジアン	rad
立体角	ステラジアン	sr

表2 SIと併用される単位

名称	記号
分, 時, 日	min, h, d
度, 分, 秒	°, ', "
リットル	l, L
トン	t
電子ボルト	eV
原子質量単位	u

$1 \text{ eV} = 1.60218 \times 10^{-19} \text{ J}$   
 $1 \text{ u} = 1.66054 \times 10^{-27} \text{ kg}$

表5 SI接頭語

倍数	接頭語	記号
$10^{18}$	エクサ	E
$10^{15}$	ペタ	P
$10^{12}$	テラ	T
$10^9$	ギガ	G
$10^6$	メガ	M
$10^3$	キロ	k
$10^2$	ヘクト	h
$10^1$	デカ	da
$10^{-1}$	デシ	d
$10^{-2}$	センチ	c
$10^{-3}$	ミリ	m
$10^{-6}$	マイクロ	$\mu$
$10^{-9}$	ナノ	n
$10^{-12}$	ピコ	p
$10^{-15}$	フェムト	f
$10^{-18}$	アト	a

表3 固有の名称をもつ SI組立単位

量	名称	記号	他のSI単位による表現
周波数	ヘルツ	Hz	$\text{s}^{-1}$
力	ニュートン	N	$\text{m} \cdot \text{kg} / \text{s}^2$
圧力, 応力	パスカル	Pa	$\text{N} / \text{m}^2$
エネルギー, 仕事, 熱量	ジュール	J	$\text{N} \cdot \text{m}$
工率, 放射束	ワット	W	$\text{J} / \text{s}$
電気量, 電荷	クーロン	C	$\text{A} \cdot \text{s}$
電位, 電圧, 起電力	ボルト	V	$\text{W} / \text{A}$
静電容量	ファラド	F	$\text{C} / \text{V}$
電気抵抗	オーム	$\Omega$	$\text{V} / \text{A}$
コンダクタンス	ジーメンズ	S	$\text{A} / \text{V}$
磁束	ウェーバ	Wb	$\text{V} \cdot \text{s}$
磁束密度	テスラ	T	$\text{Wb} / \text{m}^2$
インダクタンス	ヘンリー	H	$\text{Wb} / \text{A}$
セルシウス温度	セルシウス度	$^{\circ}\text{C}$	
光度	ルーメン	lm	$\text{cd} \cdot \text{sr}$
照射度	ルクス	lx	$\text{lm} / \text{m}^2$
放射能	ベクレル	Bq	$\text{s}^{-1}$
吸収線量	グレイ	Gy	$\text{J} / \text{kg}$
線量当量	シーベルト	Sv	$\text{J} / \text{kg}$

表4 SIと共に暫定的に維持される単位

名称	記号
オングストローム	$\text{\AA}$
バ	b
バル	bar
ガール	Gal
キュリー	Ci
レントゲン	R
ラド	rad
レム	rem

$1 \text{ \AA} = 0.1 \text{ nm} = 10^{-10} \text{ m}$   
 $1 \text{ b} = 100 \text{ fm}^2 = 10^{-28} \text{ m}^2$   
 $1 \text{ bar} = 0.1 \text{ MPa} = 10^5 \text{ Pa}$   
 $1 \text{ Gal} = 1 \text{ cm} / \text{s}^2 = 10^{-2} \text{ m} / \text{s}^2$   
 $1 \text{ Ci} = 3.7 \times 10^{10} \text{ Bq}$   
 $1 \text{ R} = 2.58 \times 10^{-4} \text{ C} / \text{kg}$   
 $1 \text{ rad} = 1 \text{ cGy} = 10^{-2} \text{ Gy}$   
 $1 \text{ rem} = 1 \text{ cSv} = 10^{-2} \text{ Sv}$

(注)

- 表1-5は「国際単位系」第5版, 国際度量衡局 1985年刊行による。ただし, 1 eV および 1 uの値は CODATA の1986年推奨値によった。
- 表4には海里, ノット, アール, ヘクタールも含まれているが日常の単位なのでここでは省略した。
- barは, JISでは流体の圧力を表わす場合に限り表2のカテゴリーに分類されている。
- EC閣僚理事会指令では bar, barn および「血圧の単位」mmHgを表2のカテゴリーに入れている。

## 換算表

力	N (=10 <sup>5</sup> dyn)	kgf	lbf
	1	0.101972	0.224809
	9.80665	1	2.20462
	4.44822	0.453592	1

粘度  $1 \text{ Pa} \cdot \text{s} (\text{N} \cdot \text{s} / \text{m}^2) = 10 \text{ P} (\text{ポアズ}) (\text{g} / (\text{cm} \cdot \text{s}))$

動粘度  $1 \text{ m}^2 / \text{s} = 10^4 \text{ St} (\text{ストークス}) (\text{cm}^2 / \text{s})$

圧	MPa (=10 bar)	kgf/cm <sup>2</sup>	atm	mmHg (Torr)	lbf/in <sup>2</sup> (psi)
	1	10.1972	9.86923	$7.50062 \times 10^3$	145.038
力	0.0980665	1	0.967841	735.559	14.2233
	0.101325	1.03323	1	760	14.6959
	$1.33322 \times 10^{-4}$	$1.35951 \times 10^{-3}$	$1.31579 \times 10^{-3}$	1	$1.93368 \times 10^{-2}$
	$6.89476 \times 10^{-3}$	$7.03070 \times 10^{-2}$	$6.80460 \times 10^{-2}$	51.7149	1

エネルギー・仕事・熱量	J (=10 <sup>7</sup> erg)	kgf·m	kW·h	cal (計量法)	Btu	ft·lbf	eV	1 cal = 4.18605 J (計量法)
	1	0.101972	$2.77778 \times 10^{-7}$	0.238889	$9.47813 \times 10^{-4}$	0.737562	$6.24150 \times 10^{18}$	= 4.184 J (熱化学)
	9.80665	1	$2.72407 \times 10^{-6}$	2.34270	$9.29487 \times 10^{-3}$	7.23301	$6.12082 \times 10^{19}$	= 4.1855 J (15 °C)
	$3.6 \times 10^6$	$3.67098 \times 10^5$	1	$8.59999 \times 10^5$	3412.13	$2.65522 \times 10^6$	$2.24694 \times 10^{25}$	= 4.1868 J (国際蒸気表)
	4.18605	0.426885	$1.16279 \times 10^{-6}$	1	$3.96759 \times 10^{-3}$	3.08747	$2.61272 \times 10^{19}$	仕事率 1 PS (仏馬力)
	1055.06	107.586	$2.93072 \times 10^{-4}$	252.042	1	778.172	$6.58515 \times 10^{21}$	= 75 kgf·m/s
	1.35582	0.138255	$3.76616 \times 10^{-7}$	0.323890	$1.28506 \times 10^{-3}$	1	$8.46233 \times 10^{18}$	= 735.499 W
	$1.60218 \times 10^{19}$	$1.63377 \times 10^{20}$	$4.45050 \times 10^{-26}$	$3.82743 \times 10^{-20}$	$1.51857 \times 10^{-22}$	$1.18171 \times 10^{-19}$	1	

放射能	Bq	Ci
	1	$2.70270 \times 10^{11}$
	$3.7 \times 10^{10}$	1

吸収線量	Gy	rad
	1	100
	0.01	1

照射線量	C/kg	R
	1	3876
	$2.58 \times 10^{-4}$	1

線量当量	Sv	rem
	1	100
	0.01	1

Abstracts of the Workshop on Orbital Ordering and Fluctuations in d- and f-electron Systems March 4-6, 2002, ASRC, JAERI, Tokai, Japan



古紙配合率100%  
白色度70%再生紙を使用しています